Available online at www.sciencedirect.com
SCIENCE DIRECT®
Physica C 398 (2003) 41–48
PHYSICA C
www.elsevier.com/locate/physc

Three-dimensional Josephson junction networks with coupling inhomogeneities in magnetic fields

A. Tuohimaa [a,b], J. Paasi [c], R. De Luca [d,*], T. Di Matteo [e,f]

[a] Finnish Defence Forces Technical Research Centre, FIN-34111 Lakiala, Finland
[b] Laboratory of Electromagnetics, Tampere University of Technology, FIN-33101 Tampere, Finland
[c] VTT Industrial Systems, VTT Technical Research Centre of Finland, P.O. Box 1306, FIN-33101 Tampere, Finland
[d] INFM and DIIMA, Università degli Studi di Salerno, Via Ponte don Melillo DIIMA, I-84084 Fisciano (SA), Italy
[e] INFM—Dipartimento di Fisica, Università degli Studi di Salerno, I-84081 Baronissi (SA), Italy
[f] Applied Mathematics, Research School of Physical Science, Australian National University, 0200 Canberra, Australia

Received 27 February 2003; received in revised form 16 May 2003; accepted 20 May 2003

Abstract

The influence of coupling inhomogeneities on the static magnetic response of a three-dimensional $8\times8\times8$ network of Josephson junctions is studied numerically. The inhomogeneities we consider are of two types. The first consists of an extended low-coupling-energy region in the network, the second is realized by taking the in-plane superconducting coupling energy ten times higher that the coupling energy between planes. The present analysis is carried out for conventional 0-junctions.

PACS: 74.50.+r; 74.25.Ha; 74.81.Fa
Keywords: Josephson effect; Magnetic properties; Granular superconductors

1. Introduction

The magnetic behaviour of one-dimensional and two-dimensional Josephson junction networks (1D, 2D-JJNs) has been extensively studied during the last decade. Indeed, the discovery of high temperature superconductivity (HTS) [1] has stimulated a large variety of studies on these systems, since it was soon realized that the low magnetic field behaviour of high-T_c superconductors could be simulated by means of JJNs [2]. Only at a later stage, it was recognized that inductances needed to be included in these models in order to properly describe shielding current effects in granular HTS materials [3,4]. The great majority of results has been obtained for homogeneous networks of conventional 0-junctions [5–7], thus accounting for the qualitative magnetic behaviour of s-wave superconducting granular systems. More recent approaches take account of d-wave symmetry in the HTS superconducting state by introducing π-junctions in the model networks [8,9]. However, the present work is carried out entirely

* Corresponding author. Tel.: +39-89-964263; fax: +39-89-964191.
E-mail address: deluca@diima.unisa.it (R. De Luca).

0921-4534/$ - see front matter
doi:10.1016/S0921-4534(03)01241-3

within the framework of conventional s-wave superconducting granular systems. In order to more closely describe the properties of this class of materials, coupling inhomogeneities in JJN models are taken into account. In this respect, the effects of spatial variation of the maximum Josephson current have been already studied using 2D-JJNs [4]. On the other hand, three-dimensional Josephson junction networks (3D-JJNs) could provide additional information on the current and flux distribution in s-wave granular materials.

In previous works we have studied the magnetic response of a single cube [10,11] and of homogeneous network of n cubes [12]. The 3D-JJN with n cubes showed an analogous behaviour to 1D- and 2D-JJNs. Indeed, the results obtained in this case confirm the existence of the critical state and of the vortex state, and also confirm that the flux pinning parameter β plays a crucial role in characterizing these states.

In the present work we shall investigate the effects of coupling inhomogeneities in 3D-JJN models. We shall here treat two cases. In the first case an extended region of Josephson coupling energy in the network is considered, in the second case the coupling Josephson energy is described by a single value of the parameter β ($\beta_x = \beta_y = 1$) for junctions lying on horizontal planes (xy-planes) and by a coupling parameter $\beta_z = 0.1$ for junctions connecting adjacent horizontal planes and lying along the vertical direction (z-axis). Therefore, in the following section we shall give a rather brief description of the analysis adopted, referring the reader to more extensive earlier work on the subject. In the third section we shall present results obtained in the two cases above and conclusions will be drawn in the last section.

2. Model

We here give a short account of the procedure followed in studying the properties of 3D-JJN models (Fig. 1) consisting of $n = n_x \times n_y \times n_z$ elementary cubic cells in the presence of a uniformly applied magnetic field **H**. Though in the present work we take $n_x = n_y = n_z = 8$, we shall nevertheless present a general description of these models.

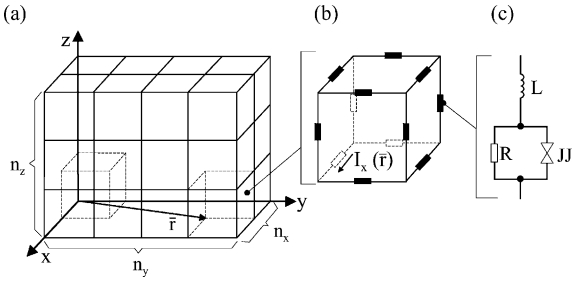

Fig. 1. Josephson junction network model. (a) Network made of $n = n_x n_y n_z$ cubes. (b) Elementary cubic Josephson junction network with current variable. (c) Box containing inductance L and ideal Josephson junction JJ, shunted with resistance R.

We start by noticing that each cell in the network of Fig. 1 contains 12 resistively shunted ideal Josephson junctions, Fig. 1(b) and (c), which are characterized by a spatially dependent maximum Josephson current $I_{J\xi}(\mathbf{r})$ and a gauge-invariant phase difference $\varphi_\xi(\mathbf{r})$, where ξ is the direction along which a junction lies in the cell and the vector $\mathbf{r}$ is an additional index representing the position of the junction (Fig. 1(a)). We denote the face passing through the point $\mathbf{r}$ and parallel to the $\mu\nu$-plane by the collection of indices $[\mathbf{r}, \mu\nu]$, where $[\mathbf{r}, \mu\nu] = [\mathbf{r}, yz]$, $[\mathbf{r}, zx]$, or $[\mathbf{r}, xy]$. The magnetic flux through the face $[\mathbf{r}, \mu\nu]$ is $\phi_{\mu\nu}(\mathbf{r})$, and the branch current flowing through a junction placed at $\mathbf{r}$ and lying in the ξ-direction is $I_\xi(\mathbf{r})$. For an overdamped junction, shunted with resistances R, the current $I_\xi(\mathbf{r})$ can be expressed as follows [13]

$$I_\xi(\mathbf{r}) = \frac{\phi_0}{2\pi R}\frac{\mathrm{d}\varphi_\xi(\mathbf{r})}{\mathrm{d}t} + I_{J\xi}(\mathbf{r})\sin\varphi_\xi(\mathbf{r}), \tag{1}$$

where ϕ_0 is the magnetic flux quantum. By means of fluxoid quantization [13], for each face in each cell of the network we can write the magnetic flux—superconducting phase difference relation as follows

$$\frac{2\pi\phi_{\mu\nu}(\mathbf{r})}{\phi_0} = \varphi_\nu(\mathbf{r}+a\hat{\boldsymbol{\mu}}) - \varphi_\nu(\mathbf{r}) - \varphi_\mu(\mathbf{r}+a\hat{\boldsymbol{\nu}}) + \varphi_\mu(\mathbf{r}), \tag{2}$$

where a is the lattice constant and where zero-field-cooling conditions are assumed. Furthermore, in order to obtain a relation between the branch currents and the magnetic flux, we can proceed as

follows: The fluxes $\phi_{\mu\nu}(\mathbf{r})$ can be calculated from the expression

$$\phi_{\mu\nu}(\mathbf{r}) = \oint \mathbf{A}(\mathbf{r}) \cdot \mathrm{d}\mathbf{l} + \mu_0 \mathbf{H} \cdot \mathbf{S}_{\mu\nu}(\mathbf{r}), \tag{3}$$

where the line integral is taken around the face $[\mathbf{r}, \mu\nu]$, and where $\mathbf{A}$ is the magnetic vector potential due to the branch currents and $\mathbf{S}_{\mu\nu}(\mathbf{r})$ is the area vector pertaining to the cube face around which we are integrating. The line integral on a single branch lying in the μ-direction ($\mathrm{d}\mathbf{l} = \widehat{\mu}\,\mathrm{d}\mu$) can be evaluated, so that

$$\int_0^a \mathbf{A}(\mathbf{r}) \cdot \mathrm{d}\mathbf{l} = \int_0^a A_\mu(\mathbf{r})\,\mathrm{d}\mu = \frac{\mu_0}{4\pi} \sum_{\mathbf{r}'} \int_0^a \int_0^a \frac{I_\mu(\mathbf{r}')}{d_{\mu,\mu'}}\,\mathrm{d}\mu\,\mathrm{d}\mu', \tag{4}$$

where $d_{\mu,\mu'}$ is the distance between the element $\mathrm{d}\mathbf{l}$ lying along the branch chosen and a generic element $\mathrm{d}\mathbf{l}'$ on any other branch in the network. By Eq. (4) we see that only those elements $\mathrm{d}\mathbf{l}'$ lying along the μ-direction need to be considered. Now, by defining the partial mutual inductance as

$$M^p_{(\mu)}(\mathbf{r}, \mathbf{r}') = \frac{\mu_0}{4\pi} \int_0^a \int_0^a \frac{\mathrm{d}\mu\,\mathrm{d}\mu'}{d_{\mu,\mu'}}, \tag{5}$$

we may rewrite Eq. (3) as follows:

$$\phi_{\mu\nu}(\mathbf{r}) = \sum_{\mathbf{r}'} \left\{ \left[M^p_{(\mu)}(\mathbf{r}, \mathbf{r}') - M^p_{(\mu)}(\mathbf{r} + a\widehat{\nu}, \mathbf{r}') \right] I_\mu(\mathbf{r}') - \left[M^p_{(\nu)}(\mathbf{r}, \mathbf{r}') - M^p_{(\nu)}(\mathbf{r} + a\widehat{\mu}, \mathbf{r}') \right] I_\nu(\mathbf{r}') \right\} + \phi^{\mathrm{ex}}_{\mu\nu}(\mathbf{r}), \tag{6}$$

where $\phi^{\mathrm{ex}}_{\mu\nu}(\mathbf{r}) = \mu_0 \mathbf{H} \cdot \mathbf{S}_{\mu\nu}(\mathbf{r})$. The partial mutual inductances can be solved analytically for one dimensional wires [12].

We notice that, since Eq. (1) can be written for all the n JJs in the network, it is representative of a set of non-linear ordinary differential equations whose initial conditions are given by the particular superconducting state realized in the network. Moreover, Eqs. (2) and (6), generally written for any position vector $\mathbf{r}$, are taken to be valid only within the network, while they reduce to a trivial equality ($0 = 0$) outside the network. In this way the boundary conditions may be imposed by setting to zero all currents outside the network. In order to obtain the magnetic flux and current distribution in the network, we start by calculating the fluxes from the phase-differences, Eq. (2), and then solve Eq. (3) for the currents in terms of the fluxes. Finally, we substitute the currents in Eq. (1), and obtain a set of coupled non-linear differential equations for the phase differences. This set of differential equations is solved using the fourth-order Runge–Kutta method with adaptive time-step. Further details on the 3D-JJN model can be found in Refs. [10,12].

3. Results

In the present section we study the magnetic response of zero-field-cooled (ZFC) networks numerically. The external magnetic field is increased in small increments in order to simulate realistic magnetic field sweeps. For computational purposes, we define a normalized external flux $\psi_{\mathrm{e}} = 2\pi\phi_{\mathrm{e}}/\phi_0$, where $\phi_{\mathrm{e}} = \mu_0 H a^2$, and a flux pinning capacity parameter $\beta = 2\pi l I_{\mathrm{J}}/\phi_0$, where l is the partial self inductance of a branch [12] and I_{J} is the maximum Josephson current taken without the indices ξ and $\mathbf{r}$. In this way, the inhomogeneity can be introduced through the adimensional parameter β by letting I_{J} vary over the network branches; the partial mutual inductance, however, is considered to remain unaltered. Notice also that, even though the parameter β should be written as a function of ξ and $\mathbf{r}$, in the present analysis we use β without extra notation for simplicity.

After each increase $\Delta\psi_{\mathrm{e}} = 0.05\pi$ of the external normalized flux ψ_{e}, the system is allowed to relax close to its stationary solution with an integration time $\Delta t = 100\ l/R$, where l/R is the natural time unit of the JJN (about 10^{-10}–10^{-12} s). The computed values of the magnetic flux and current distributions are recorded and stored before the external magnetic field is increased again.

In the following, we shall examine flux penetration mainly in the loops (or faces) parallel to the xy-plane. These loops form layers characterized by the ratio $k = r_z/a$, which defines the vertical position of the layer in space. The directions of the magnetic fields are chosen in such a way that the flux distribution in xz- and yz-layers can be

deduced from the one shown for the *xy*-layers. For example, when the external field **H** is applied along the *z*-direction, we see that, for a homogeneous network, the flux lines are aligned along **H** and the dark spots, denoting local presence of magnetic flux, appear to have the same size and to be placed in the same position in the layers (see Fig. 2(a)). Notice that the values representing the normalized magnetic flux multiplied by 2π are given in grey-colour scales at the bottom of each figure. On the other hand, when inhomogeneity is introduced in the coupling parameters, these spots may change in size and be displaced, on the *xy*-plane, with respect to the upper or lower ones. In this case, it is arguable that the flux lines are bent and that non-null local magnetic flux appear in one or both of the remaining coordinate planes. Thus we show the flux distribution in *xy*-faces and cut off the other faces for simplicity. However, when the flux distribution in the other faces, for example the *yz*-layers, is not immediately clear from the flux distribution in *xy*-layers, we provide a second figure, which contains the flux distribution in *yz*-layers, cutting off the other faces. Furthermore, the spacing of the layers represented in Figs. 2–7 is larger than the actual spacing between layers in the network for the sake of clarity.

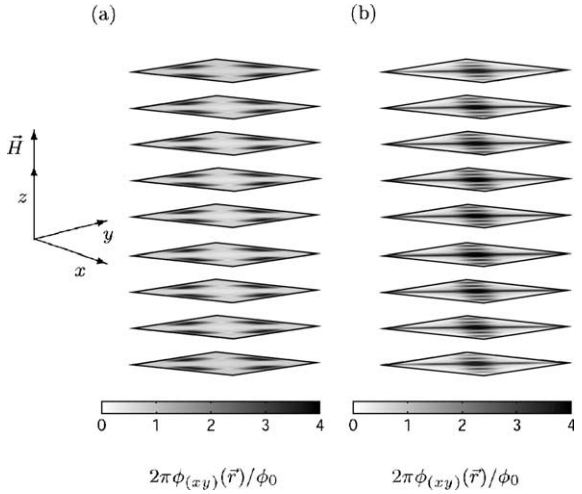

Fig. 2. Magnetic flux distribution in the *xy*-layers of a homogeneous $8\times8\times8$ network with $\beta = 1$, (a) for $\psi_e = 0.7\pi$, and (b) for the remanent state ($\psi_e = 0$). $\widehat{H} = \{0, 0, 1\}$.

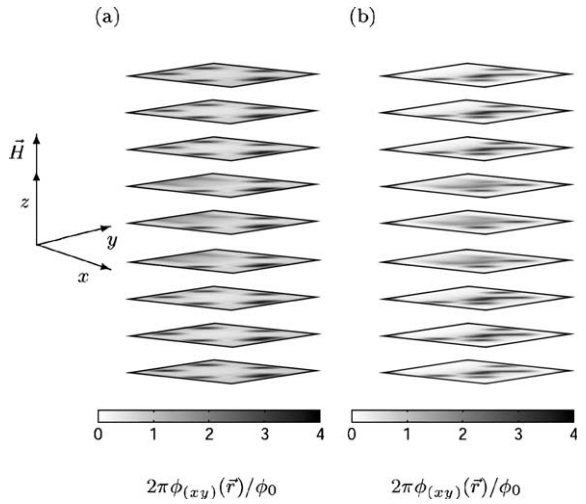

Fig. 3. Magnetic flux distribution in the *xy*-layers of an inhomogeneous $8\times8\times8$ network with $\beta = 1$, (a) for $\psi_e = 0.7\pi$, (b) and for the remanent state ($\psi_e = 0$). The inhomogeneity is a low-j_c region with $\beta = 0.1$ located in the portion of the network enclosed by the branches for which the index $i = r_x/a$ ranges from 2 to 5, the index $j = r_y/a$ ranges from 0 to 4, and the index $k = r_z/a$ ranges from 4 to 6, where $r = (r_x, r_y, r_z)$ denotes the position of the branch and where the limiting branches are included in the the low-j_c region. $\widehat{H} = \{0, 0, 1\}$.

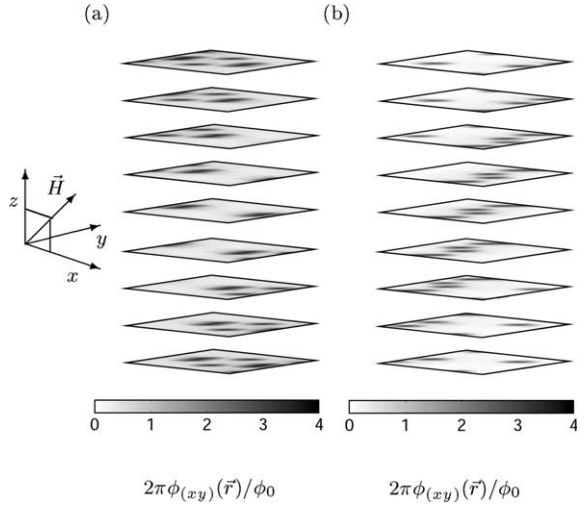

Fig. 4. Magnetic flux distribution in the *xy*-layers of a homogeneous $8\times8\times8$ network with $\beta = 1$ (a) for $\psi_e = 0.7\pi$, and (b) for the remanent state ($\psi_e = 0$). $\widehat{H} = \{1/\sqrt{2}, 0, 1/\sqrt{2}\}$.

In the present paper we focus our attention on the influence of coupling inhomogeneities, char-

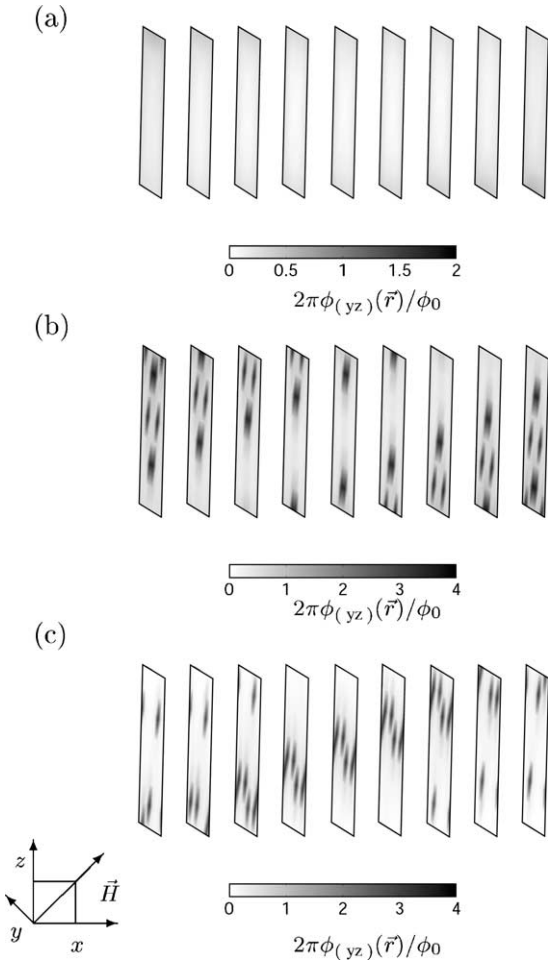

Fig. 5. Magnetic flux distributions in the yz-layers of a homogeneous $8\times8\times8$ network with $\beta = 1$, (a) for $\psi_e = 0.4\pi$, (b) for $\psi_e = 0.7\pi$, and (c) for the remanent state ($\psi_e = 0$). $\widehat{H} = \{1/\sqrt{2}, 0, 1/\sqrt{2}\}$.

acterized by low critical current density j_c, on the magnetic flux distribution of 3D-JJNs. As specified before, the network size is $8\times8\times8$, which is large enough to show the characteristic behaviour of these systems. In all cases the external magnetic flux is at first swept up from zero to $\psi_e = 4\pi$ and then decreased down to $\psi_e = 0$. We chose to use parameter values $\beta = 1$ and $\beta = 0.1$, which are suitable for showing inhomogeneity effects on the same scale of the size of a Josephson network vortex.

Let us first study the response of a homogeneous 3D-JJN, when the magnetic field is applied

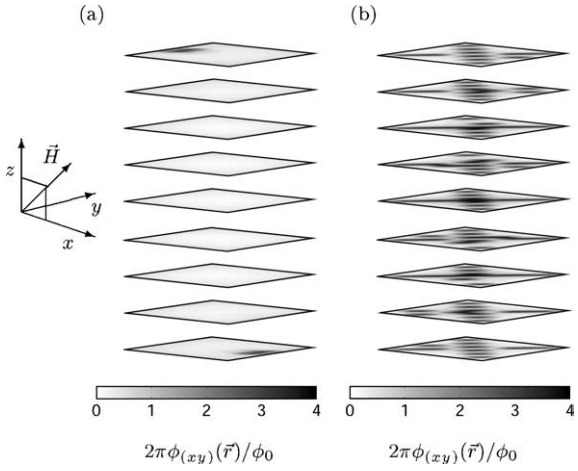

Fig. 6. Magnetic flux distribution in the xy-layers of a inhomogeneous $8\times8\times8$ network with $\beta_x = \beta_y = 1$, and $\beta_z = 0.1$, (a) for $\psi_e = 0.7\pi$, and (b) for the remanent state ($\psi_e = 0$). $\widehat{H} = \{1/\sqrt{2}, 0, 1/\sqrt{2}\}$.

along the z-axis. In Fig. 2(a) the magnetic flux distribution is reported for the external flux value $\psi_e = 0.7\pi$, which is just above the lower threshold normalized flux of the JJN, ψ_{th}, defined as the value of the normalized external flux at which first irreversible penetration takes place. The value of ψ_{th} can be obtained by observing, for increasing values of the applied normalized flux ψ_e, through small increments $\Delta\psi_e$, for which value of ψ_e nonzero values of the magnetic flux could be first detected in the remanent state. Here, the Josephson network vortices penetrate into the sample identically from each side. Notice that in Fig. 2(a) flux lines gather in four regions closer to the midpoints of the four sides in each layer. As the field increases, more vortices move into the sample. After the maximum value $\psi_e = 4\pi$ is reached, the external flux is decreased and some network vortices flow out of the system. Finally, at zero field ($\psi_e = 0$) the remanent flux distribution shown in Fig. 2(b) is obtained. In Fig. 2(b) the flux patterns on the two diagonals are equal, even though it does not clearly appear from the picture.

Having obtained the magnetic flux distribution in the homogeneous network, we may study the effect of the presence of low-j_c regions in an $8\times8\times8$ JJN with $\beta = 1$. In Fig. 3 we report the flux distribution in this type of network, presenting

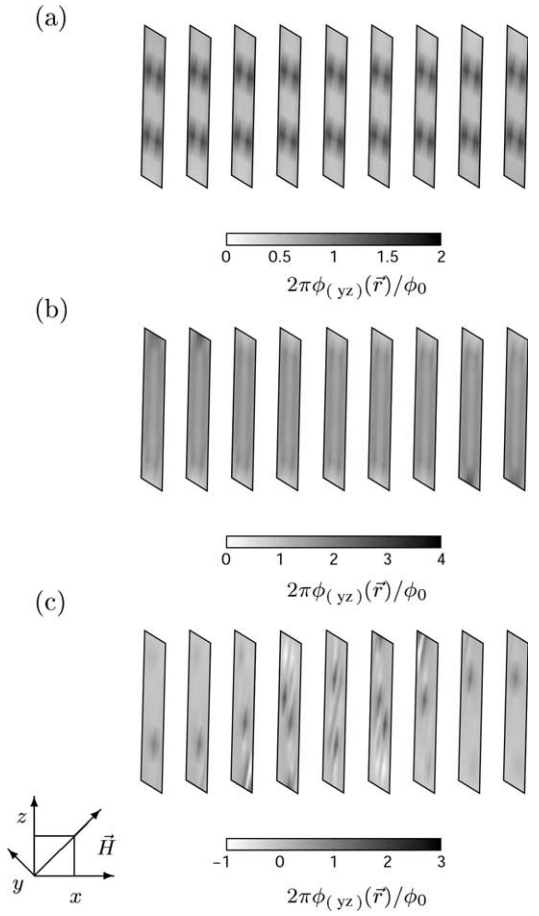

Fig. 7. Magnetic flux distributions in the yz-layers of an inhomogeneous $8\times8\times8$ network with $\beta_x = \beta_y = 1$, and $\beta_z = 0.1$, (a) for $\psi_e = 0.4\pi$, (b) for $\psi_e = 0.7\pi$, and (c) for the remanent state ($\psi_e = 0$). $\widehat{H} = \{1/\sqrt{2}, 0, 1/\sqrt{2}\}$.

a low-j_c region with $\beta = 0.1$ in the network portion where the index $i = r_x/a$ ranges from 2 to 5, the index $j = r_y/a$ ranges from 0 to 4, and the index $k = r_z/a$ ranges from 4 to 6. Thus, in the low-j_c region, I_J is ten times lower than in the $\beta = 1$ region. As it can be seen from Fig. 2(a), in the homogeneous network the vortices tend to be straight, since the flux pattern is not altered from layer to layer. The same can be noticed for the outer layers in Fig. 3(a), where $\psi_e = 0.7\pi$: The vortices are straight and their magnetic moments tend to be parallel to the external field. However, in the middle layers ($k = 4, 5, 6$), where the low-j_c region is present, the magnetic flux is distributed over a larger area than in the $\beta = 1$ layers. This is in agreement with the network penetration depth being inversely proportional to the square root of the critical current density [6,7]. Therefore, except for the flux spreading effect appearing in the $\beta = 0.1$ region, the flux distribution for $\psi_e = 0.7\pi$ is quite similar to that of the homogeneous network with $\beta = 1$. The same can be noted for the remanent magnetic flux distribution reported in Fig. 3(b): The flux distribution is similar to that of the homogeneous network in Fig. 2(a), except for the portion of the network where the low-j_c region is present. It is therefore clear that the magnetic flux trapping capacity of the network is lower in the low-j_c region, so that this region may work as a bridge for the magnetic flux to enter and leave the network.

Let us now study the response of the system when the magnetic field is applied in the direction $\widehat{H} = \{1/\sqrt{2}, 0, 1/\sqrt{2}\}$. Magnetic flux distribution of a homogeneous $8\times8\times8$ network with $\beta = 1$ is shown for the xy-layers in Fig. 4, and for the yz-layers in Fig. 5. The external flux values are $\psi_e = 0.4\pi$ in Fig. 5(a), $\psi_e = 0.7\pi$ in Figs. 4(a) and 5(b). In Figs. 4(b) and 5(c) ψ_e is brought back to $\psi_e = 0$. From Fig. 5(a) we notice that the magnetic flux has not irreversibly penetrated into the sample. The lower threshold normalized flux in this case is just above 0.4π, which qualitatively agrees with lower threshold field results of a single cube [11]. As it can be seen from Figs. 4(a) and 5(b), at $\psi_e = 0.7\pi$ several vortices, with magnetic moments parallel to the external field, have entered the sample. Furthermore, the flux distributions in the xy-layers are similar to the corresponding ones for yz-layers, as one would expect. In the remanent state, Figs. 4(b) and 5(c), some magnetic flux is trapped in the innermost cells lying along the direction parallel to the external field direction. Other vortices are present elsewhere in the network, appearing to be slightly bent. Notice, finally, how the overall magnetic flux distribution in the xy-layers (Fig. 4(a) and (b)) results quite different from those obtained for $\widehat{H} = \{0, 0, 1\}$ and reported in Fig. 2(a) and (b).

The above results were presented also to allow comparison with the case, which we shall consider next, where the junctions lying in the x- or y-

directions have a maximum Josephson current I_J ten times higher than those lying on the z-direction. The corresponding β values are $\beta_x = \beta_y = 1$ and $\beta_z = 0.1$. In Figs. 6 and 7 the magnetic flux distribution of the inhomogeneous network is reported for the xy-layers and the yz-layers, respectively. As before, the external flux values are $\psi_e = 0.4\pi$ for Fig. 7(a), $\psi_e = 0.7\pi$ for Figs. 6(a) and 7(b), and $\psi_e = 0$ for Figs. 6(b) and 7(c). From Fig. 7(a) we see that, at $\psi_e = 0.4\pi$, the magnetic flux has already penetrated the inner region of the JJN, in the form of Josephson network vortices through the yz-layers, but not through the xy-layers (Fig. 6(a)). Thus these Josephson network vortices have magnetic moments parallel to the x-direction. Notice also that penetrated vortices in the yz-layers spread over regions having smaller dimensions in the z-direction than in the y-direction, as visible from Fig. 7(a). With increasing fields more vortices penetrate into the yz-layers through the weak junctions lying in z-direction. These vortices may reduce or increase the net current flowing in the outermost junctions and thus, in general, the magnetic flux may enter into the xy-layers at different external flux values than in the homogeneous case discussed above. Indeed, in the case at hand, we need to specify two different lower threshold fluxes: one for the x-direction, $\psi_{th,x} = 0.35\pi$–0.4π, and another for the z-direction, $\psi_{th,z} = 0.65\pi$–0.7π. Therefore, at $\psi_e = 0.7\pi$ the Josephson network vortex has just penetrated into the uppermost and downmost xy-layers, Fig. 6(a), whereas in the yz-layers magnetic flux is fully penetrated, Fig. 7(b). The remanent magnetic flux distribution in the xy-layers, Fig. 6(b), is quite similar to that of Fig. 2(b), and most of the vortices seen in the xy-layers have magnetic moments parallel to the z-direction. The only visible difference is given by a few additional vortices which lie in the same direction as the external field, Fig. 7(c), and go through the xy-layers, Fig. 6(b). Therefore, the average remanent magnetization is not parallel to $\hat{H}$ in this case.

From the viewpoint of granular materials, these results indicate that intergranular vortices may be bent and the area occupied by one vortex may locally vary. Thus intergranular vortices are elastic, in the sense of collective pinning theory, cf. [14]. It is finally important to notice that, while the network size used in the present work might still allow us to draw conclusions on some features of the magnetic response of these superconducting systems, as, for instance, the presence of intergranular critical state [12], a full quantitative analysis should take into account the actual extension of the sample and would thus result in excessively long and complex numerical computations.

4. Conclusions

The low-field magnetic response of an $8\times8\times8$ inhomogeneous three-dimensional network of Josephson junctions is studied numerically. Two types of inhomogeneities were considered, the first being an extended low-coupling-energy region in the network, the second being given by an anisotropic type of coupling for which the in-plane superconducting coupling energy is ten times higher that the coupling energy between planes. Moreover, two different field orientations, one along the z-direction, one forming an angle of $\pi/4$ with the z-axis, are chosen to investigate the magnetic response of the system.

The results show that a non-uniform coupling between adjacent junctions introduce the characteristic feature of magnetic flux bending. Indeed, when an extended region of low-coupling energy is introduced in the homogeneous network and the resulting flux distribution in the network layers is shown for various external field values, the network vortices are seen to spread over a larger area in the low-coupling-energy region. In this way the flux lines are necessarily bent inside the system. Moreover, when the coupling parameters β_ξ ($\xi = x, y, z$) are chosen to give an overall anisotropic coupling of the Josephson junctions in the network ($\beta_x = \beta_y = 1$ and $\beta_z = 0.1$), the system is seen to show different threshold fields. Thus, for applied fields not parallel to the z-axis, the flux lines may penetrate the lateral layers of the network more easily, so that, even in this case, the flux lines are bent, inside the system, with respect to the external field direction.

As for possible applications of the present analysis to the study of the magnetic behaviour of

s-wave superconducting granular specimens, we may say that inhomogeneities in the JJN model can mimic the variation of the coupling energy between adjacent grains. Therefore, extrapolating these results to the case of superconducting granular systems, where the interstitial regions between grains act as pinning centers with characteristic barrier energy of the order of the Josephson coupling energy, we notice that the presence of low-j_c regions in the sample may degrade its shielding and pinning properties, if at least one border of this region coincides with the external border of the sample. In this case, indeed, Josephson junctions with low I_J values are located in the peripheral part of the network and the threshold field is lowered. This allows irreversible flux penetration in the system at lower applied field magnitudes and an easier escape route for flux lines when the normalized applied flux ψ_e is lowered down to zero, where the remanent state is realized.

Finally, we may notice that only by extending the present analysis to larger systems a behaviour quantitatively closer to the magnetic response of granular superconductors could be approached. However, the characteristic feature of magnetic flux bending, obtained with the present analysis, is expected to remain unaltered. Nevertheless, in order to perform flux penetration simulations in real specimens, massive computation would be needed and, even if it were possible to produce such a great amount of calculations, this effort would still not be sufficient to give a full quantitative description of the static magnetic response of superconducting granular systems. In fact, in order to attain the goal of a full quantitative description of the magnetic properties of granular superconductors, one should also account for the magnetic response of the superconducting grains, which in JJN systems are simply taken to be point-like objects. Aiming at this goal poses new challenges to researchers in the field, but surely opens new fascinating perspectives for the future.

Acknowledgements

The authors wish to express their gratitude to Dr. A. Majhofer at Warsava University, Poland for useful discussions.

References

[1] K.A. Müller, G. Bednorz, Science 237 (1987) 1133.
[2] J.R. Clem, Physica C 153–155 (1988) 50.
[3] R. De Luca, S. Pace, B. Savo, Phys. Lett. A 154 (1991) 185.
[4] J. Paasi, A. Tuohimaa, J.-T. Eriksson, Physica C 259 (1996) 10.
[5] D.-X. Chen, J.J. Moreno, A. Sanchez, Phys. Rev. B 53 (1996) 6579;
D.-X. Chen, A. Sanchez, A. Hernando, Physica C 250 (1995) 107;
D.-X. Chen, A. Sanchez, Phys. Rev. B 50 (1994) 13735.
[6] D. Dominguez, J. José, Phys. Rev. B 53 (1996) 11692.
[7] A. Majhofer, T. Wolf, W. Dieterich, Phys. Rev. B 44 (1991) 9634;
A. Majhofer, Physica B 222 (1996) 273.
[8] A. Tuohimaa, J. Paasi, T. Di Matteo, Inst. Phys. Conf. Ser. 167 (2000) 771.
[9] V.K. Kornev, I.V. Borisenko, P.B. Mozhaev, G.A. Ovsyannikov, N.F. Pedersen, Physica C 367 (2002) 285.
[10] R. De Luca, T. Di Matteo, A. Tuohimaa, J. Paasi, Phys. Rev. B 57 (1998) 1173.
[11] T. Di Matteo, A. Tuohimaa, J. Paasi, R. De Luca, Phys. Lett. A 247 (1998) 360.
[12] A. Tuohimaa, J. Paasi, T. Tarhasaari, T. Di Matteo, R. De Luca, Phys. Rev. B 61 (2000) 9711.
[13] A. Barone, G. Paternò, Physics and Applications of Josephson Effect, Wiley, New York, 1982.
[14] G. Blatter, M.V. Feigel'man, V.B. Geshkenbein, A.I. Larkin, V.M. Vinokur, Rev. Mod. Phys. 66 (1994) 1125.